HHS Public Access

Author manuscript

Mol Pharm. Author manuscript; available in PMC 2016 July 06.

Published in final edited form as:

Mol Pharm. 2015 July 6; 12(7): 2517–2527. doi:10.1021/acs.molpharmaceut.5b00035.

Phagocytosed Clofazimine Biocrystals can Modulate Innate Immune Signaling by Inhibiting TNFα and Boosting IL-1RA Secretion

Gi S. Yoon[a], **Sudha Sud**[a], **Rahul K. Keswani**[a], **Jason Baik**[a,#], **Theodore J. Standiford**[b], **Kathleen A. Stringer**[c], and **Gus R. Rosania**[a,*]

[a]Department of Pharmaceutical Sciences, University of Michigan College of Pharmacy, Ann Arbor, MI 48109, USA

[b]Division of Pulmonary and Critical Care Medicine, Department of Internal Medicine, University of Michigan, School of Medicine, Ann Arbor, MI 48109 USA

[c]Department of Clinical, Social and Administrative Sciences, University of Michigan, College of Pharmacy, Ann Arbor, MI 48109, USA

Abstract

Clofazimine (CFZ) is an FDA-approved leprostatic and anti-inflammatory drug that massively accumulates in macrophages, forming insoluble, intracellular crystal-like drug inclusions (CLDIs) during long-term oral dosing. Interestingly, when added to cells *in vitro*, soluble CFZ is cytotoxic because it depolarizes mitochondria and induces apoptosis. Accordingly, we hypothesized that *in vivo*, macrophages detoxify CFZ by sequestering it in CLDIs. To test this hypothesis, CLDIs of CFZ-treated mice were biochemically isolated, and then incubated with macrophages *in vitro*. The cell biological effects of phagocytosed CLDIs were compared to those of soluble CFZ. Unlike soluble CFZ, phagocytosis of CLDIs did not lead to mitochondrial destabilization or apoptosis. Rather, CLDIs altered immune signaling response pathways downstream of Toll-like receptor (TLR) ligation, leading to enhanced interleukin-1 receptor antagonist (IL-1RA) production, dampened NF-κB activation and tissue necrosis factor alpha (TNFα) production, and ultimately decreased TLR expression levels. In aggregate, our results constitute evidence that macrophages detoxify soluble CFZ by sequestering it in a biocompatible, insoluble form. The altered cellular response to TLR ligation suggests that CLDI formation may also underlie CFZ's anti-inflammatory activity.

Keywords

biocompatibility; cell signaling; drug delivery; immunomodulation; liquid crystal; macrophage

[*]Corresponding author: Tel: 734-763-1032. Fax: 734-615-6162. grosania@umich.edu.
[#]Now at Optivia Biotechnology Inc., 115 Constitution Dr. Menlo Park, CA 94025

Supporting Information Available

The following file is available at the ACS Publications website free of charge.

File name: Supplemental Information. Supplementary materials and methods, and figures S1–S4.

Conflict of Interest

Gus R. Rosania is a consultant for Bristol Myers-Squibb. The authors have no other conflicts of interest to declare.

Introduction

Clofazimine (CFZ) is an FDA-approved anti-mycobacterial agent recommended by the World Health Organization as part of the standard treatment of leprosy.[1,2] It has been in clinical use since the 1960s, and is well-tolerated, although bioaccumulation of the drug can lead to visible (but reversible) changes in skin pigmentation.[3,4] In mice, CFZ forms intracellular, crystal-like drug inclusions (CLDIs) upon prolonged oral administration.[5] These CLDIs are exclusively present in macrophages, such as bone marrow macrophages, peritoneal macrophages and Kupffer cells.[5] CLDI formation is attributed to the drug's lipophilicity (logP>7) and low aqueous solubility.[6] CLDI formation may account for some of the drug's unusual pharmacokinetic properties, including a long half-life following an acute dose[7,8] which increases further during prolonged, chronic treatment.[9–11]

Interestingly, CLDIs have also been documented in humans following autopsies and toxicological case studies of CFZ-treated patients.[12–15] While the drug is FDA-approved for clinical use, there have been no scientific studies examining the toxicological properties of CLDIs, or any other biologically-derived insoluble drug complex. Although the formation of insoluble drug precipitates or crystals inside cells could be readily dismissed as an unwanted side effect, CLDI formation is intrinsically linked to the drug's macrophage targeting mechanism, as well as its downstream pharmacological and toxicological effects. Furthermore, CLDIs can function as intracellular drug depots, accounting for the drug's prolonged elimination half-life, as well as the fact that mycobacteria have not developed resistance to CFZ in spite of decades of clinical use. Perhaps more importantly, to the extent that CLDIs may influence macrophage-dependent immune signaling functions, they could be one of the reasons why CFZ is also clinically useful as an anti-inflammatory agent for the treatment of various inflammatory disorders.[16–22] From a biomaterials and nanotechnology perspective, the presence of CLDIs in the cells of human patients clearly illustrates how it is possible to endow cells with artificial structural and functional elements, using self-assembling, orally bioavailable small molecule building blocks. CLDIs possess nanoscale structural features, with properties resembling liquid crystals.[5] Furthermore, CLDIs are fluorescent and their fluorescence can change in response to the surrounding microenvironment. Structurally, they are bounded by a membrane of likely biological origin[5] and they are mostly composed of protonated CFZ molecules in a chloride salt form[23] (reference 23 submitted to *Molecular Pharmaceutics*; included with this manuscript as Supporting Information for Review Only). Because they are already present in the cells of human patients treated with CFZ, the many interesting chemical, physical and biological properties of CLDIs could serve as a starting point for developing new kinds of CFZ-based solid-state nano-derivatives with potential applications in diagnostics, drug delivery and therapeutics.

Accordingly, we aimed to establish the ability of CLDIs to alter innate immune signaling in macrophages following phagocytosis *in vitro*, in the context of the reported apoptosis-inducing properties of soluble CFZ on cultured macrophages.[24] While apoptosis can serve as an anti-inflammatory mechanism,[25–27] there is no evidence that CFZ induces macrophage apoptosis *in vivo*. Therefore, we also decided to compare the *in vitro* CLDI-induced changes

in Toll-like receptor (TLR)-dependent pro- and anti-inflammatory signaling pathways, in relation to those of freely soluble CFZ. Experimentally, we used the macrophage-derived Raw 264.7 cells as an experimental model. Considering both the amount of CFZ added to the cells as well as the cell-associated CFZ content allowed equitable comparison of intracellular CLDIs with those of freely soluble CFZ. Following phagocytosis of CLDIs, we proceeded to analyze the associated changes in cell viability, mitochondrial integrity, and inflammatory signaling pathways downstream of TLRs which play a critical role in inflammation, innate immune response as well as in the initiation of adaptive immune responses.[28–31]

Materials and Methods

Reagents

All primary antibodies were purchased from Cell Signaling Technology (Danvers, MA), except p65 and TLR4 (Abcam, UK), actin and TLR2 (Sigma, St. Louis, MO), and TLR9 (Thermo Pierce, Rockford, IL). Pam3 and LPS were purchased from Invivogen (San Diego, CA).

Purification of CFZ crystal-like drug inclusions (CLDIs) from mice spleen and CFZ quantification

Clofazimine (Sigma-Aldrich, C8895) was prepared in sesame oil (Shirakiku, Japan, or Roland, China) and Powdered Lab Diet 5001 (PMI International, Inc., St. Louis, MO) and orally administrated to C57BL6 mice (4 week old, Jackson Laboratory, Bar Harbor, ME) for 8 weeks as previously described.[5,9] The animal protocol was approved by the University of Michigan's Animal Care and Use Committee in accordance with the National Institutes of Health guidelines (UCUCA #PRO0005111).

Spleens were harvested and CLDIs were isolated using a previously described method with some modifications.[5] The spleens were cut into small pieces, homogenized with a syringe plunger and then filtered through a 40 μm cell strainer to remove connective tissue debris. The spleen homogenate was centrifuged (300 × g for 10 min) to remove large cell debris and the pelleted CLDIs were resuspended in 10% sucrose in Dulbecco's PBS (DPBS) without $CaCl_2$ and $MgCl_2$, pH 7.4. CLDIs were further purified using a 3-layer discontinuous gradient (50%, 30% and 10% sucrose in DPBS) centrifugation method (3200 × g for 30 min). For incubation with RAW 264.7 cells, CLDIs were washed 3 times with DPBS to remove sucrose and resuspended in DMEM with 5% FBS. Protein concentration of purified CLDI isolates before and after gradient centrifugation and subsequent washing with DPBS was determined using the bicinchoninic acid detection (BCA) assay (Thermo Pierce). CFZ content was spectrophotometrically measured using a previously described method with some modifications.[6,9] CLDIs in DPBS (100 μl of sample) were mixed with equal volume of xylene to create lipid-aqueous partitioning and then vortexed to dissolve CLDIs and extract the CFZ into the organic phase. The CFZ-containing xylene was placed into a new tube. Fresh xylene was added to the sample and the process was repeated twice until there was no CFZ remaining in the aqueous phase. The CFZ content in xylene was extracted twice using equal volume of 2.5 M H_2SO_4 and vortexing until there was no CFZ remaining in xylene.

Final CFZ concentration was calculated from the standard curve generated by adding a known amount of drug solution to 2.5 M H_2SO_4 and measurement of absorbance at 530nm (Synergy-2 plate reader; Biotek, Winooski, VT). The average extraction yield of CFZ was 90%, with elimination of 99% of protein.

Culture of RAW 264.7 cells with soluble CFZ or CLDIs and TLR stimulation

The murine macrophage cell line RAW 264.7 was purchased from ATCC (Manassas, VA) and maintained in DMEM (Life Technologies, Carlsbad, CA) supplemented with 10% FBS. Soluble CFZ or isolated CLDIs were added at various concentrations in DMEM with 5% FBS to 6-well plates containing 4 x 10^5 cells/well and incubated (24 h at 37°C and 5% CO_2). Culture supernatants were harvested at 24 h, centrifuged (1500 × g for 5 min), and stored (−20°C) in frozen aliquots prior to analysis. For experiments involving TLR stimulation, cells were washed twice with pre-warmed DPBS to remove extracellular, non-phagocytosed CLDIs or CFZ, and then the cells were serum-starved for 18 h in DMEM. Supernatants were collected from unstimulated cells and cells stimulated with 200 ng/ml Pam3 or 1 μg/ml LPS in DMEM.

CLDI Phagocytosis assay

The ability of RAW 264.7 cells to phagocytose CLDIs was measured by incubating cells with increasing concentrations of CLDIs for 24 h, as described above. The cells were then washed twice with pre-warmed PBS to remove extracellular CLDIs and images were captured using the Nikon Eclipse Ti (Japan) inverted microscope with brightfield to count cells and fluorescence at Cy5 wavelength to count CLDIs. Cells and CLDIs from each image were manually counted to calculate the percentage of CLDI-containing cells and the mean number of CLDIs internalized by each cell. A minimum of 5 random images were analyzed for each concentration (minimum 640 total cells counted). CLDI internalization was confirmed by confocal microscopy, following labeling of the plasma membrane of cells with the lipophilic, fluorescent styryl probe FM-143.

Live cell staining and imaging

Cells were cultured with CFZ or CLDI media for 24 h in chamber slides (Lab Tek) and stained with 150 nM of MitoTracker Red CMXRos (MTR, Life Technologies) in fresh media for 45 min, and then NucBlue Live Cell Stain (Life Technologies) was applied for 10 min for nuclear staining. After incubation, extracellular MTR and NucBlue were washed twice with DPBS and the cells were visualized on a Nikon Eclipse Ti fluorescence microscope (Japan) using Texas Red (Mitotracker) and DAPI (NucBlue) filters. Real-time live cell images were captured every 10 sec for 30 min with the same microscope and video was created using the Nikon Elements software. For confocal imaging of intracellular CLDIs, FM 1-43 (Life Technologies) was used at 3.5 μM (15 min at 37 °C) for membrane staining followed by NucBlue (10 min). After washing with DPBS, cells were visualized using laser-scanning confocal microscopy (Olympus Fluoview 500) fitted with argon (FITC) and HeNe Red lasers (Cy5). Images were taken along the z-axis with a 60x objective at 0.25 μm intervals and the composite Z-stack images were created using the Nikon Elements software.

Microscopy and image analysis

Brightfield and fluorescence (DAPI, FITC, Texas Red and Cy5) images were captured using the Nikon Eclipse Ti (Japan) inverted microscope equipped with a Nikon Digital Sight DS-Fi2 camera (Japan) for brightfield and Photometrics Coolsnap Myo camera (Tucson, AZ) for fluorescence. Polarized images were acquired with CRi Abrio Imaging System (Hinds Instruments, Hillsboro, OR) fitted on the same microscope with a 623nm polarizing filter using the OpenPolScope plugin for ImageJ and Micro-Manager.[32] For determining the ratio of nucleus-to-cytoplasm p65 fluorescence, ImageJ was used following previously described methods.[33,34] The average volume of CLDIs was calculated using the area, Feret max and min values of each CLDI acquired from ImageJ. Each CLDI was considered to be cylindrical in shape. A detailed diagram of the calculation method is shown in supplemental figures (Fig. S1).

Cell viability assay (XTT assay)

Cells were plated in triplicate wells at a density of 5×10^3 per well in 96-well plates in DMEM with 5% FBS and allowed to adhere overnight. Soluble CFZ (Stock solution 5mM in DMSO) or CLDIs were added (0.25, 0.5, 1, 2, 4, 10, 20, 40 and 80 μM final concentrations) to cells and incubated (37°C) for 24 h. XTT assay (Roche, UK) was carried out according to the manufacturer's instructions with absorbance measured at 450 nm and 690 nm using a Synergy-2 plate reader (Biotek). The cell viability percentage was calculated by comparing absorbance of CFZ and CLDI-treated cells to control (untreated) cells.

TNFα and IL-1RA ELISA

The media of cells with or without 6 h TLR stimulation by Pam3 or LPS was harvested, and TNFα and IL-1RA levels were measured by ELISA (Duoset, R&D Systems, Minneapolis, MN) in duplicate wells according to the manufacturer's instructions. The cytokine concentrations were expressed as picogram per milligram of cell lysate. Experiments were repeated three times and values are expressed as the mean ± SD.

Isolation of alveolar macrophages

CFZ- or control chow-fed mice were euthanized by exsanguination while deeply anesthetized by intraperitoneal injection of 300μl ketamine/xylazine. The trachea was surgically exposed and cannulated with an 18G needle and the lungs were lavaged by instilling DPBS containing 0.5 mM EDTA in 1 ml aliquots for a total of 6 ml. Approximately 90% of the bronchoalveolar lavage (BAL) was retrieved. BAL was then centrifuged for 10 min at 400 x *g*, 4°C and resuspended in RPMI 1640 media (Life Technologies). The cells were placed in 12-well culture plate (Corning, Tewksbury, MA) and washed with media after 45 min, enabling the isolation of alveolar macrophages by adherence. The cells were imaged in brightfield and lysed in RIPA buffer (Sigma) for Western blot.

Data processing and statistics

All data were expressed as mean ± standard deviation. Statistical analysis was performed with one-way analysis of variance (ANOVA) and Bonferroni's post-hoc comparisons, or

with Student's t-test (paired, two-way). Correlation analyses were performed using a Pearson's correlation coefficient measurement. All statistical analyses employed the IBM SPSS software and $p \leq 0.05$ was considered statistically significant.

Results

1. Clofazimine CLDI purification from spleen

In order to obtain pure CLDIs we elaborated a method to isolate and purify CLDIs from the spleen of 8wk CFZ-fed mice using a 3-layer discontinuous gradient centrifugation method. Brightfield, polarized and fluorescence microscopy images (Fig. 1A) were acquired before and after gradient centrifugation to characterize and detect any alterations in the physiochemical properties of CLDIs, including crystal structure or chemical composition.[5] As seen through polarized light microscopy, diattenuation at 623nm, slow axis orientation and transmittance was maintained in CLDIs after the isolation process, indicative of the preservation of the crystal structure of CLDIs. The CFZ molecule is inherently fluorescent at Texas Red and FITC channels, but the protonation and chlorination of CFZ, as is the case with CLDIs, can cause spectral shifts to Texas Red- and Cy5-positive, but FITC-negative wavelengths.[5,35] Therefore, fluorescence microscopy enables the detection of changes in the morphology of CLDIs, as well as changes in the microenvironment surrounding CFZ molecules in CLDIs.

Comparing the optical properties of CLDIs before and after the purification process thus showed that CLDIs were not altered by the purification process. The size dimensions of spleen CLDIs displayed as rod-shaped crystals (Fig. 1A) had an average area of 9.96±8.66 (SD) μm^2 and Feret dimensions of 7.01±3.59 μm (max) and 1.66±0.74 μm (min) prior to gradient centrifugation (Fig. 1B). The average volume was 17.08±27.27 μm^3 before gradient centrifugation. Size analysis showed a heterogeneous population of CLDIs, evidenced by high standard deviations of average area and calculated volume (Fig. 1B), with at least 96% of CLDIs smaller than 30 μm^2 before gradient centrifugation (Fig. 1C). The purification process removed many of the smaller CLDIs ranging from 0–5 μm^2, but enriched those over 10 μm^2 (Fig. 1C), and thus increasing the average area and volume of CLDIs to 13.29±9.73 μm^2 and 24.57±35.42 μm^3, respectively, and Feret dimensions to 8.28±3.57 μm (max) and 1.88±0.82 μm (min) (Fig. 1B). Most importantly, no degradation, fragmentation, aggregation or other gross morphological changes in the properties of CLDIs were observed during the purification process.

2. Active phagocytosis of CLDIs by RAW 264.7 cells

The red color of CFZ allowed monitoring the cellular uptake of soluble CFZ or CLDIs (Fig. 2A). In some of the cells (10–15%), we observed CLDIs inside vacuole-like intracellular vesicles (Fig. 2A inset image). As shown in Figure 2B, 16.7±4.3% and 28.6±5.1% of the cells showed evidence of CLDI uptake at 2.5μM and 5μM concentrations, respectively, without obvious differences in the number of CLDIs per cell (1.58±0.35 and 1.66±0.16). With increasing doses, we observed a dose-dependent increase in the percentage of cells with CLDIs as well as the number of CLDIs per cell. At 40μM, the maximal dose tested, 89.6±3.22% of cells averaged 3.22±0.29 CLDIs per cell (Fig. 2B). The phagocytic index

(percentage of CLDI positive cells × mean number of CLDIs per cell), which measures the ability of macrophages to phagocytose particles,[36] was highly correlated between CLDI concentration and CLDI phagocytosis (Supplemental fig. S2). To confirm that CLDIs were internalized, we conducted confocal microscopy and Z-stacking, which clearly demonstrated the cytoplasmic localization of CLDIs (Fig. 2C). A real-time video of CLDI phagocytosis by a RAW 264.7 cell is shown in supplemental figure S3. Penetration or damage of the plasma membrane or cell nucleus by CLDIs was not observed.

3. Intracellular CLDIs are not cytotoxic

CLDIs induced minimal cytotoxicity (Fig. 3A) even at very high concentrations (81% viability at 40 μM), but soluble CFZ exerted cytotoxicity at a 20-fold lower concentration (61% viability at 2μM). Exposure of RAW 264.7 cells to soluble CFZ at 10μM reduced cell viability to 20%, whereas CLDIs at the same concentration maintained cell viability at 80% (Fig. 3A). Intracellular CLDIs also did not affect mitochondrial membrane potential (Fig. 3B), as seen from the staining of the membrane potential-sensitive (Mitotracker Red; MTR) fluorescent probe. However, macrophages treated with soluble CFZ exhibited diffuse cytoplasmic MTR staining, indicative of mitochondrial membrane depolarization, and displayed fewer mitochondria labeled with MTR. Morphological evidence of apoptosis, such as membrane blebbing, was only seen in soluble CFZ-treated cells (Fig. 3B, arrowhead). MTR signal intensity of the nuclear area was measured to quantify MTR leakage, which was similar in CLDI-treated cells and untreated cells, whereas soluble CFZ-treated cells displayed increased nuclear MTR signal by 4-fold (Fig. 3C).

Changes in mitochondrial membrane permeability such as those leading to difference in MTR staining are upstream of activation of apoptosis pathways mediated by activation of caspases, proteolysis of caspase substrates, and ultimately leading to cell death. Since previous studies also indicated that soluble CFZ could activate apoptosis pathways in cultured macrophages,[24] we proceeded to directly establish the activation of apoptotic pathways by monitoring caspase-3 and PARP cleavage after CFZ or CLDI treatment. Indeed, while soluble CFZ caused increased PARP cleavage at low concentrations (4 and 10 μM; Fig. 3D), CLDIs did not induce caspase-3 activation or PARP cleavage, even at the highest concentrations (80μM).

4. Intracellular CLDIs activate the Akt pathway and enhance IL-1RA production

Previous studies on mice fed with a CFZ-supplemented diet for an 8 week period indicated increased levels of interleukin 1 receptor antagonist (IL-1RA) an endogenous, secreted anti-inflammatory signaling molecule.[9] Thus, we proceeded to establish whether CFZ or CLDIs boosted IL-1RA secretion by cultured macrophages. Remarkably, while soluble CFZ did not affect IL-1RA secretion, phagocytosed CLDIs significantly enhanced the production of IL-1RA in a concentration dependent manner (Fig. 4A). Phosphorylation of Akt, which marks the activation of the signal transduction pathway leading to upregulation of IL-1RA expression[28,37,38] also was increased in concentration-dependent manner in cells that phagocytosed CLDIs. Solubilized CFZ minimally affected phosphorylation of Akt with no effect on IL-1RA expression (Fig. 4B).

5. Intracellular CLDIs dampen TLR2- and TLR4-mediated NF-κB activation and TNFα production

Next, we tested whether soluble CFZ or CLDIs were able to activate pro-inflammatory signaling pathways by monitoring the secretion of TNFα from the cultured cells. Soluble CFZ or CLDIs failed to induce TNFα production on their own (Fig. 5A). Thus, we proceeded to determine if CFZ or CLDIs would promote TNFα release if the cells were pre-stressed with pro-inflammatory stimuli. Surprisingly, both soluble CFZ and CLDIs suppressed TLR2- and 4-mediated inflammatory responses and decreased TNFα production, IκB phosphorylation (p-IκB), and NF-κB (p65) nuclear translocation (Fig. 5) following ligation of TLRs. Ingested CLDIs inhibited TNFα production in response to Pam3 (TLR2) and LPS (TLR4) stimulation at 10 (Pam3, 55.6%; LPS, 52.3%), 20 (Pam3, 67.6%; LPS, 72.1%) and 40μM (Pam3, 82.9%; LPS, 89.5%) concentrations (Fig. 5A). In contrast, soluble CFZ only inhibited LPS stimulated TNFα at 2 (51.2%) and 4μM (76.5%) concentrations, while Pam3/TLR2-mediated TNFα production was not affected (Fig. 5A).

In order to further understand the mechanisms leading to TNFα inhibition, we measured IκB phosphorylation (Fig. 5B) and NF-κB (p65) nuclear translocation (Fig. 5C–G). Phosphorylation of IκB leads to the release of bound NF-κB complex, followed by its nuclear translocation and transcription of TNFα and other pro-inflammatory genes. In accordance with TNFα assay results, we observed reduced p-IκB levels in response to Pam3 and LPS stimulation in CLDI-containing cells in a concentration-dependent manner (Fig. 5B). Moreover, soluble CFZ only inhibited LPS/TLR4-mediated IκB phosphorylation, while the Pam3/TLR2-mediated response was not affected. Furthermore, by monitoring the nuclear and cytoplasmic distribution of intracellular NF-κB (p65) in soluble CFZ or CLDI-containing cells with or without Pam3 or LPS stimulation (Fig. 5C–E), and by comparing the ratio of nuclear to cytoplasmic p65 staining intensity, we were able to measure the ability of CLDIs to reduce both LPS and Pam3-induced nuclear translocation of p65 (Fig. 5G). Soluble CFZ (4μM) reduced p65 translocation in response to LPS, but not Pam3 (Fig. 5G). In addition, the presence of intracellular soluble CFZ or CLDIs alone did not induce nuclear translocation of p65 (Fig. 5G, naïve), and the reduction of p65 nuclear translocation in CLDI-containing cells correlated with the measured reduction in p-IκB levels (Fig. 5B, G).

Inhibition of IκB phosphorylation and NF-κB activation could be achieved by interference with multiple points upstream of the signaling pathway so we assayed for TLR2, TLR4 and TLR9 levels, as well as the adaptor molecule MyD88. Interestingly, increasing concentrations of CLDI treatment led to decreased levels of TLR2 and TLR4 expression following 24 h incubation (Fig. 5H). Conversely, soluble CFZ upregulated TLR2 and TLR4 expression over the same time period. The expression of intracellular TLR9 or MyD88 was not changed in both soluble CFZ and CLDI treated cells. Western blot data were confirmed by immunofluorescence microscopy, which showed downregulation of TLR2 and TLR4, but not TLR9 in CLDI-containing cells (Supplemental figure S4).

In order to verify whether the accumulation of soluble CFZ or CLDIs altered TLR2 expression in mice, primary alveolar macrophages (AM) from mice fed with control chow or CFZ for 4 wks (which are loaded with soluble CFZ but not CLDIs) or 8 wks (which

contain CLDIs) (Fig. 5I) were subjected to Western blot detection of TLR2. Relative to untreated controls, TLR2 expression was moderately increased in soluble CFZ-containing AMs obtained from 4 wk treated animals. More importantly, TLR2 was downregulated in CLDI-containing AMs obtained from 8 wk treated animals (Fig. 5J).

Discussion

To summarize our experimental results, cultured macrophages incubated with soluble CFZ exhibit evidence of impaired mitochondrial function, activation of apoptotic pathways and decreased cell viability. However, cells containing phagocytosed CLDIs exerted profoundly different changes in intracellular signal transduction pathways downstream of TLR2 and TLR4 ligation, ultimately leading to downregulation of TLR2 and TLR4 expression on the cell surface, and an associated decrease in TNFα production while boosting IL-1RA release. These findings demonstrate that CLDIs can affect immunomodulatory pathways without altering mitochondrial integrity, promoting apoptosis or decreasing cell viability. Furthermore, when compared to untreated cells or to cells treated with soluble CFZ, phagocytosed CLDIs resulted in changes in Akt phosphorylation, and inhibition of NF-κB (p65) signaling downstream of TLR receptor ligation, which are directly related to the observed increase in IL-1RA release and reduction in TNFα production.

Underscoring the significance of these results, there have been many clinical reports indicating that CFZ possesses anti-inflammatory and immunosuppressive activities, evident in various cutaneous, non-microbial and chronic inflammatory disorders, including discoid lupus erythematosus,[16,17] pustular psoriasis,[18] Melkersson–Rosenthal syndrome,[19] necrobiosis lipoidica and granuloma annulare,[20] as well as cutaneous lesions in systemic lupus erythematosus.[21] Topical application of CFZ has been shown to exhibit anti-inflammatory effects on tuberculoid leprosy.[22] More recent studies have explored expanding the indication of CFZ to non-cutaneous inflammatory disorders such as multiple sclerosis, rheumatoid arthritis and type I diabetes mellitus.[2] Despite this known anti-inflammatory activity, the molecular and cellular mechanisms that underlie this property of CFZ have not been elucidated. Although it had been reported that soluble CFZ causes mitochondrial membrane destabilization and activation of caspase 9-mediated apoptosis in epithelial cells and macrophages *in vitro*,[6,24] CFZ does not behave as the typical, apoptosis-inducing immunosuppressive agent. This is because unlike other cytotoxic, immunosuppressive drugs (e.g., methotrexate, azathioprine or cyclosporine), CFZ is well tolerated and safe *in vivo* even when administered at very high doses for prolonged periods of time.[5] Furthermore, *in vivo* studies indicate that CLDIs are present inside viable macrophages with no evidence of cytotoxicity.[9] Therefore, while our observations do not completely exclude the possibility that macrophage apoptosis may contribute to the suppression and resolution of inflammation,[25–27] they indicate that CLDIs can activate alternative immunomodulatory pathways in macrophages.

Because CLDIs naturally accumulate within resident tissue macrophages in mice and humans, it can be inferred that CLDIs serve to decrease the toxicity of CFZ.[9] Thus, CLDIs can be considered as a fundamental component of an intrinsically biocompatible detoxification system. Based on these experiments, the main cellular effect of CLDIs is that

macrophages acquire a more anti-inflammatory, wound-healing phenotype, characterized by down regulation of TLR2 and TLR4-mediated, innate immune signaling pathways which can result in cells being less responsive to pro-inflammatory stimuli. This is consistent with CFZ being a safe, well-tolerated drug.

The finding that soluble CFZ and CLDIs differentially modulate IL-1RA and TLR-induced TNFα production *in vitro* indicates that the macrophage targeted bioaccumulation of CFZ may be the key to understanding its *in vivo* anti-inflammatory function. In macrophages and other cell types, TLRs function as pattern recognition receptors, responsible for induction of innate immune responses against a wide variety of pathogens. Following TLR ligation, the immune response of the organism is controlled by the balance between pro-inflammatory and anti-inflammatory signals, of which TNFα and IL-1RA play crucial roles. Although the precise mechanism by which CLDIs exert their effect on TLR-signaling pathways remains to be fully elucidated, one possibility is that the phagocytosis of CLDIs, but not soluble CFZ, could be triggering TLR activation at a low level that fails to produce a robust inflammatory response, but can transiently reprogram the cell to become desensitized or hyporesponsive towards a subsequent stronger TLR challenge.[39] Also, one can imagine that different effects of soluble CFZ and CLDIs may be partly due to differences in how alternate forms of the drug interact with cellular membranes, with soluble CFZ associated with an increased propensity to destabilize cellular membranes while forming disordered drug-membrane aggregates.[6]

With regards to the specific, cellular signaling pathways affected by soluble CFZ compared with CLDIs, intracellular CLDIs by themselves did not trigger TNFα expression or NF-κB nuclear translocation. Soluble CFZ treatment did not lead to altered TNFα secretion in Pam3-stimulated cells even though TLR2 expression was increased. This could be due to either unchanged MyD88 expression or the effect of soluble CFZ on cell viability, which may affect cell signaling. However, LPS-elicited TNFα secretion was significantly dampened, which may implicate soluble CFZ as a specific inhibitor for the TLR4 induced inflammatory response. Several publications have highlighted lipids, such as fatty acids and high-density lipoprotein (HDL) can dampen TLR4 signaling and NF-kB activation.[40–42] In addition, TLR4 requires additional accessory molecules such as MD2, CD36, and TRAIL for full activation of signaling pathways, whereas TLR2/1 signaling does not.[43] Thus, it is possible that soluble CFZ may interfere with the interaction of TLR4 with these accessory molecules.

A more unique aspect of the biocompatibility and anti-inflammatory activity of CLDIs are the increased activation of the Akt pathway and enhanced production of IL-1RA, which is not evident when cells are treated with soluble CFZ. For the first time, our results demonstrate that enhanced IL-1RA expression is specifically caused by the presence of intracellular CLDIs, which leads to direct effects on the PI-3K/Akt pathway which controls IL-1RA expression levels.[37,44] This is also an important finding because IL-1RA is a cytokine that inhibits the activity of IL-1β, which is one of the main pro-inflammatory cytokines in chronic inflammatory diseases.[45] By competing with IL-1β for the same receptor, IL-1RA is critical for the resolution of inflammation and wound healing.[45] CLDIs, seem to have no effect on 1L-1β expression or inflammasome activation. In our previous

studies in mice orally administered with CFZ for 8 weeks, CLDIs were found to massively accumulate in the lung, liver and spleen. As a marker of inflammasome activation, we could not find changes in IL-1β expression in these organs compared to control diet-fed age-matched mice.[9] Therefore, we do not have any indication that CLDIs induce inflammasome activation, as has been observed with monosodium urate[46] or cholesterol[47] crystals.

In terms of the clinical significance of these observations, TNFα is a critical inflammatory mediator in the pathogenesis of local or systemic inflammatory diseases. Several drugs currently on the market act by decreasing TNFα levels or interfering with its activity. These drugs are used to treat inflammatory bowel diseases,[48] rheumatoid arthritis,[49,50] and psoriasis.[51,52] Furthermore, recombinant human IL-1RA is also clinically used as a drug (anakinra/Kineret; Sobi, Sweden) to treat rheumatoid arthritis. It has also been shown to reduce airway inflammation[53] and is being considered for the treatment of inflammatory lung diseases, including acute respiratory distress syndrome,[54] acute lung injury,[55–57] allergic airway inflammation,[58] and bronchopulmonary dysplasia.[59] As an added note, down-regulation of TLRs could also contribute to CFZ's activity against mycobacteria. For instance, mycobacterial components have been reported to engage with TLR2, TLR4 and TLR9 in macrophages to trigger pro-inflammatory responses.[60,61] Clinical studies have shown that TLR2 and 4 are downregulated in leprosy patients undergoing successful corticosteroid therapy, which may contribute to the reversal reaction of leprosy.[62]

During the past 10 years, TLRs have emerged as a major class of pro-inflammatory mediators in mammals and humans.[63] Recognition of pathogen-associated molecular patterns by TLRs, either alone or in heterodimerization with other TLR or non-TLR receptors, triggers pro-inflammatory signaling pathways through adaptors MyD88 and/or TRIF, which then leads to increased production and release of TNFα, IL-1RA, as well as other cytokines and chemokines responsible for the activation of innate and adaptive immune responses.[63] Because TLRs can exert profound effects on the immune system,[30,64,65] TLR signaling must be tightly regulated to prevent inappropriate or over-activation that might cause damaging inflammation to the host.[66,67] While TLRs have emerged as a promising therapeutic target for the treatment of inflammation,[68] these results indicate that formulation of CFZ into CLDI-like complexes could be useful for modulating TLR-dependent inflammatory disease processes.

Conclusions

To conclude, our findings demonstrate the unique immunomodulatory effects of CLDIs on TLR-dependent TNFα downregulation and IL-1RA augmentation and implicate the existence of anti-inflammatory signaling pathways stemming from the formation and intracellular sequestration of insoluble, biocrystalline CFZ complexes in macrophages. In addition, CLDIs undergo active phagocytosis without causing cytotoxicity and can effectively modulate cell surface TLR expression and function. In this context, we envision that formulation of CFZ or other drugs as insoluble, CLDI-like complexes may be readily justifiable as a novel, cell type-specific, macrophage-targeted therapeutic approach for treating inflammatory diseases.

Supplementary Material

Refer to Web version on PubMed Central for supplementary material.

Acknowledgments

This study was supported by NIH grant R01GM078200 (GRR) and the University of Michigan MCubed Initiative (http://mcubed.umich.edu/). The authors thank Avery Lui for help with image analysis.

References

1. Barry VC, Belton JG, Conalty ML, Denney JM, Edward DW, O'Sullivan JF, Twomey D, Winder F. A New Series of Phenazines (rimino-Compounds) with High Antituberculosis Activity. Nature. 1957; 179:1013–1015. [PubMed: 13430770]
2. Cholo MC, Steel HC, Fourie PB, Germishuizen WA, Anderson R. Clofazimine: Current Status and Future Prospects. J Antimicrob Chemother. 2012; 67:290–298. [PubMed: 22020137]
3. Atkinson AJ, Sheagren JN, Rubio JB, Knight V. Evaluation of B.663 in Human Leprosy. Int J Lepr Other Mycobact Dis. 35:119–127. [PubMed: 5338956]
4. Mansfield RE. Tissue Concentrations of Clofazimine (B663) in Man. Am J Trop Med Hyg. 1974; 23:1116–1119. [PubMed: 4429181]
5. Baik J, Rosania GR. Macrophages Sequester Clofazimine in an Intracellular Liquid Crystal-like Supramolecular Organization. PLoS One. 2012; 7:e47494. [PubMed: 23071814]
6. Baik J, Rosania GR. Molecular Imaging of Intracellular Drug-Membrane Aggregate Formation. Mol Pharm. 2011; 8:1742–1749. [PubMed: 21800872]
7. Schaad-Lanyi Z, Dieterle W, Dubois JP, Theobald W, Vischer W. Pharmacokinetics of Clofazimine in Healthy Volunteers. Int J Lepr Other Mycobact Dis. 1987; 55:9–15. [PubMed: 3559339]
8. Lu Y, Zheng M, Wang B, Fu L, Zhao W, Li P, Xu J, Zhu H, Jin H, Yin D, Huang H, Upton AM, Ma Z. Clofazimine Analogs with Efficacy against Experimental Tuberculosis and Reduced Potential for Accumulation. Antimicrob Agents Chemother. 2011; 55:5185–5193. [PubMed: 21844321]
9. Baik J, Stringer Ka, Mane G, Rosania GR. Multiscale Distribution and Bioaccumulation Analysis of Clofazimine Reveals a Massive Immune System-Mediated Xenobiotic Sequestration Response. Antimicrob Agents Chemother. 2013; 57:1218–1230. [PubMed: 23263006]
10. Levy L. Pharmacologic Studies of Clofazimine. Am J Trop Med Hyg. 1974; 23:1097–1109. [PubMed: 4611255]
11. Holdiness MR. Clinical Pharmacokinetics of Clofazimine. A Review. Clin Pharmacokinet. 1989; 16:74–85. [PubMed: 2656045]
12. Harbeck RJ, Worthen GS, Lebo TD, Peloquin CA. Clofazimine Crystals in the Cytoplasm of Pulmonary Macrophages. Ann Pharmacother. 1999; 33:250. [PubMed: 10084424]
13. Lewis JT, Candelora JN, Hogan RB, Briggs FR, Abraham SC. Crystal-Storing Histiocytosis due to Massive Accumulation of Charcot-Leyden Crystals: A Unique Association Producing Colonic Polyposis in a 78-Year-Old Woman with Eosinophilic Colitis. Am J Surg Pathol. 2007; 31:481–485. [PubMed: 17325492]
14. Jadhav MV, Sathe AG, Deore SS, Patil PG, Joshi NG, Joghi NG. Tissue Concentration, Systemic Distribution and Toxicity of Clofazimine--an Autopsy Study. Indian J Pathol Microbiol. 2004; 47:281–283. [PubMed: 16295502]
15. Desikan KV, Ramanujam K, Ramu G, Balakrishnan S. Autopsy Findings in a Case of Lepromatous Leprosy Treated with Clofazimine. Lepr Rev. 1975; 46:181–189. [PubMed: 1186410]
16. Lo JS, Berg RE, Tomecki KJ. Treatment of Discoid Lupus Erythematosus. Int J Dermatol. 1989; 28:497–507. [PubMed: 2684876]
17. Mackey JP, Barnes J. Clofazimine in the Treatment of Discoid Lupus Erythematosus. Br J Dermatol. 1974; 91:93–96. [PubMed: 4851057]

18. Chuaprapaisilp T, Piamphongsant T. Treatment of Pustular Psoriasis with Clofazimine. Br J Dermatol. 1978; 99:303–305. [PubMed: 708598]
19. Podmore P, Burrows D. Clofazimine--an Effective Treatment for Melkersson-Rosenthal Syndrome or Miescher's Cheilitis. Clin Exp Dermatol. 1986; 11:173–178. [PubMed: 3720016]
20. Arbiser JL, Moschella SL. Clofazimine: A Review of Its Medical Uses and Mechanisms of Action. J Am Acad Dermatol. 1995; 32:241–247. [PubMed: 7829710]
21. Medeiros Bezerra EL, Pereira Vilar MJ, Da Trindade Neto PB, Sato EI. Double-Blind, Randomized, Controlled Clinical Trial of Clofazimine Compared with Chloroquine in Patients with Systemic Lupus Erythematosus. Arthritis Rheum. 2005; 52:3073–3078. [PubMed: 16200586]
22. Venkateswarlu B, Venkataramana D, Rao AV, Prabhakar MC, Reddy BM. Role of Rifampin and Clofazimine Ointments in the Treatment of Leprosy. Int J Lepr Other Mycobact Dis. 1992; 60:269–270. [PubMed: 1522368]
23. Keswani RK, Baik J, Yeomans L, Hitzman C, Pawate A, Kenis PJ, Rodriguez-Hornedo N, Stringer KA, Rosania GR. Chemical Analysis of Drug Biocrystals: A Role for Counterion Transport Pathways in Intracellular Drug Disposition. Mol Pharm Submitt. 2015
24. Fukutomi Y, Maeda Y, Makino M. Apoptosis-Inducing Activity of Clofazimine in Macrophages. Antimicrob Agents Chemother. 2011; 55:4000–4005. [PubMed: 21690278]
25. Savill J. Apoptosis in Resolution of Inflammation. J Leukoc Biol. 1997; 61:375–380. [PubMed: 9103222]
26. Marriott HM, Hellewell PG, Cross SS, Ince PG, Whyte MKB, Dockrell DH. Decreased Alveolar Macrophage Apoptosis Is Associated with Increased Pulmonary Inflammation in a Murine Model of Pneumococcal Pneumonia. J Immunol. 2006; 177:6480–6488. [PubMed: 17056580]
27. Henson PM, Bratton DL. Antiinflammatory Effects of Apoptotic Cells. J Clin Invest. 2013; 123:2773–2774. [PubMed: 23863635]
28. Troutman TD, Bazan JF, Pasare C. Toll-like Receptors, Signaling Adapters and Regulation of the pro-Inflammatory Response by PI3K. Cell Cycle. 2012; 11:3559–3567. [PubMed: 22895011]
29. Drexler SK, Foxwell BM. The Role of Toll-like Receptors in Chronic Inflammation. Int J Biochem Cell Biol. 2010; 42:506–518. [PubMed: 19837184]
30. Takeuchi O, Akira S. Pattern Recognition Receptors and Inflammation. Cell. 2010; 140:805–820. [PubMed: 20303872]
31. Kawai T, Akira S. The Role of Pattern-Recognition Receptors in Innate Immunity: Update on Toll-like Receptors. Nat Immunol. 2010; 11:373–384. [PubMed: 20404851]
32. Mehta SB, Shribak M, Oldenbourg R. Polarized Light Imaging of Birefringence and Diattenuation at High Resolution and High Sensitivity. J Opt. 2013; 15
33. Fuseler JW, Merrill DM, Rogers JA, Grisham MB, Wolf RE. Analysis and Quantitation of NF-kappaB Nuclear Translocation in Tumor Necrosis Factor Alpha (TNF-Alpha) Activated Vascular Endothelial Cells. Microsc Microanal. 2006; 12:269–276. [PubMed: 17481363]
34. Noursadeghi M, Tsang J, Haustein T, Miller RF, Chain BM, Katz DR. Quantitative Imaging Assay for NF-kappaB Nuclear Translocation in Primary Human Macrophages. J Immunol Methods. 2008; 329:194–200. [PubMed: 18036607]
35. Keswani RK, Rosania GR. No Title. Unpubl. results.
36. Magenau A, Benzing C, Proschogo N, Don AS, Hejazi L, Karunakaran D, Jessup W, Gaus K. Phagocytosis of IgG-Coated Polystyrene Beads by Macrophages Induces and Requires High Membrane Order. Traffic. 2011; 12:1730–1743. [PubMed: 21883764]
37. Molnarfi N, Gruaz L, Dayer JM, Burger D. Opposite Regulation of IL-1 and Secreted IL-1 Receptor Antagonist Production by Phosphatidylinositide-3 Kinases in Human Monocytes Activated by Lipopolysaccharides or Contact with T Cells. J Immunol. 2006; 178:446–454. [PubMed: 17182583]
38. Rehani K, Wang H, Garcia CA, Kinane DF, Martin M. Toll-like Receptor-Mediated Production of IL-1Ra Is Negatively Regulated by GSK3 via the MAPK ERK1/2. J Immunol. 2009; 182:547–553. [PubMed: 19109187]
39. Morris MC, Gilliam EA, Li L. Innate Immune Programing by Endotoxin and Its Pathological Consequences. Front Immunol. 2015; 5

40. Cheng AM, Handa P, Tateya S, Schwartz J, Tang C, Mitra P, Oram JF, Chait A, Kim F. Apolipoprotein A-I Attenuates Palmitate-Mediated NF-κB Activation by Reducing Toll-like Receptor-4 Recruitment into Lipid Rafts. PLoS One. 2012; 7:e33917. [PubMed: 22479476]
41. Kim K, Jung N, Lee K, Choi J, Kim S, Jun J, Kim E, Kim D. Dietary Omega-3 Polyunsaturated Fatty Acids Attenuate Hepatic Ischemia/reperfusion Injury in Rats by Modulating Toll-like Receptor Recruitment into Lipid Rafts. Clin Nutr. 2013; 32:855–862. [PubMed: 23395256]
42. Wong SW, Kwon MJ, Choi AMK, Kim HP, Nakahira K, Hwang DH. Fatty Acids Modulate Toll-like Receptor 4 Activation through Regulation of Receptor Dimerization and Recruitment into Lipid Rafts in a Reactive Oxygen Species-Dependent Manner. J Biol Chem. 2009; 284:27384–27392. [PubMed: 19648648]
43. Lee CC, Avalos AM, Ploegh HL. Accessory Molecules for Toll-like Receptors and Their Function. Nat Rev Immunol. 2012; 12:168–179. [PubMed: 22301850]
44. Carpintero R, Brandt KJ, Gruaz L, Molnarfi N, Lalive PH, Burger D. Glatiramer Acetate Triggers PI3Kδ/Akt and MEK/ERK Pathways to Induce IL-1 Receptor Antagonist in Human Monocytes. Proc Natl Acad Sci U S A. 2010; 107:17692–17697. [PubMed: 20876102]
45. Dinarello CA, Simon A, van der Meer JWM. Treating Inflammation by Blocking Interleukin-1 in a Broad Spectrum of Diseases. Nat Rev Drug Discov. 2012; 11:633–652. [PubMed: 22850787]
46. Shi Y, Mucsi AD, Ng G. Monosodium Urate Crystals in Inflammation and Immunity. Immunol Rev. 2010; 233:203–217. [PubMed: 20193001]
47. Grebe A, Latz E. Cholesterol Crystals and Inflammation. Curr Rheumatol Rep. 2013; 15:313. [PubMed: 23412688]
48. Magro F, Portela F. Management of Inflammatory Bowel Disease with Infliximab and Other Anti-Tumor Necrosis Factor Alpha Therapies. BioDrugs. 2010; 24(Suppl 1):3–14. [PubMed: 21175228]
49. Maini R, St Clair EW, Breedveld F, Furst D, Kalden J, Weisman M, Smolen J, Emery P, Harriman G, Feldmann M, Lipsky P. Infliximab (chimeric Anti-Tumour Necrosis Factor Alpha Monoclonal Antibody) versus Placebo in Rheumatoid Arthritis Patients Receiving Concomitant Methotrexate: A Randomised Phase III Trial. ATTRACT Study Group. Lancet. 1999; 354:1932–1939. [PubMed: 10622295]
50. Lethaby A, Lopez-Olivo MA, Maxwell L, Burls A, Tugwell P, Wells GA. Etanercept for the Treatment of Rheumatoid Arthritis. Cochrane database Syst Rev. 2013; 5:CD004525. [PubMed: 23728649]
51. Gall JS, Kalb RE. Infliximab for the Treatment of Plaque Psoriasis. Biologics. 2008; 2:115–124. [PubMed: 19707434]
52. Kivelevitch D, Mansouri B, Menter A. Long Term Efficacy and Safety of Etanercept in the Treatment of Psoriasis and Psoriatic Arthritis. Biologics. 2014; 8:169–182. [PubMed: 24790410]
53. Hernandez ML, Mills K, Almond M, Todoric K, Aleman MM, Zhang H, Zhou H, Peden DB. IL-1 Receptor Antagonist Reduces Endotoxin-Induced Airway Inflammation in Healthy Volunteers. J Allergy Clin Immunol. 2014
54. Meyer NJ, Feng R, Li M, Zhao Y, Sheu CC, Tejera P, Gallop R, Bellamy S, Rushefski M, Lanken PN, Aplenc R, O'Keefe GE, Wurfel MM, Christiani DC, Christie JD. IL1RN Coding Variant Is Associated with Lower Risk of Acute Respiratory Distress Syndrome and Increased Plasma IL-1 Receptor Antagonist. Am J Respir Crit Care Med. 2013; 187:950–959. [PubMed: 23449693]
55. Grailer JJ, Canning BA, Kalbitz M, Haggadone MD, Dhond RM, Andjelkovic AV, Zetoune FS, Ward PA. Critical Role for the NLRP3 Inflammasome during Acute Lung Injury. J Immunol. 2014; 192:5974–5983. [PubMed: 24795455]
56. Hudock KM, Liu Y, Mei J, Marino RC, Hale JE, Dai N, Worthen GS. Delayed Resolution of Lung Inflammation in Il-1rn−/− Mice Reflects Elevated IL-17A/granulocyte Colony-Stimulating Factor Expression. Am J Respir Cell Mol Biol. 2012; 47:436–444. [PubMed: 22592923]
57. Ischenko AM, Nikolaev BP, Kotova TV, Vorobeychikov EV, Konusova VG, Yakovleva LY. IL-1 Receptor Antagonist as an Aerosol in Inflammation. J Aerosol Med. 2007; 20:445–459. [PubMed: 18158717]

58. Ritter M, Straubinger K, Schmidt S, Busch DH, Hagner S, Garn H, Prazeres da Costa C, Layland LE. Functional Relevance of NLRP3 Inflammasome-Mediated Interleukin (IL)-1β during Acute Allergic Airway Inflammation. Clin Exp Immunol. 2014; 178:212–223. [PubMed: 24943899]

59. Nold MF, Mangan NE, Rudloff I, Cho SX, Shariatian N, Samarasinghe TD, Skuza EM, Pedersen J, Veldman A, Berger PJ, Nold-Petry CA. Interleukin-1 Receptor Antagonist Prevents Murine Bronchopulmonary Dysplasia Induced by Perinatal Inflammation and Hyperoxia. Proc Natl Acad Sci U S A. 2013; 110:14384–14389. [PubMed: 23946428]

60. Basu J, Shin DM, Jo EK. Mycobacterial Signaling through Toll-like Receptors. Front Cell Infect Microbiol. 2012; 2:145. [PubMed: 23189273]

61. Kleinnijenhuis J, Oosting M, Joosten LaB, Netea MG, Van Crevel R. Innate Immune Recognition of Mycobacterium Tuberculosis. Clin Dev Immunol. 2011; 2011:405310. [PubMed: 21603213]

62. Walker SL, Roberts CH, Atkinson SE, Khadge S, Macdonald M, Neupane KD, Ranjit C, Sapkota BR, Dhakal S, Hawksworth RA, Mahat K, Ruchal S, Hamal S, Hagge DA, Lockwood DNJ. The Effect of Systemic Corticosteroid Therapy on the Expression of Toll-like Receptor 2 and Toll-like Receptor 4 in the Cutaneous Lesions of Leprosy Type 1 Reactions. Br J Dermatol. 2012; 167:29–35. [PubMed: 22348338]

63. Chang ZL. Important Aspects of Toll-like Receptors, Ligands and Their Signaling Pathways. Inflamm Res. 2010; 59:791–808. [PubMed: 20593217]

64. Yoon GS, Dong C, Gao N, Kumar A, Standiford TJ, Yu FSX. Interferon Regulatory Factor-1 in Flagellin-Induced Reprogramming: Potential Protective Role of CXCL10 in Cornea Innate Defense against Pseudomonas Aeruginosa Infection. Invest Ophthalmol Vis Sci. 2013; 54:7510–7521. [PubMed: 24130180]

65. Kovach MA, Standiford TJ. Toll like Receptors in Diseases of the Lung. Int Immunopharmacol. 2011; 11:1399–1406. [PubMed: 21624505]

66. Qian C, Cao X. Regulation of Toll-like Receptor Signaling Pathways in Innate Immune Responses. Ann N Y Acad Sci. 2013; 1283:67–74. [PubMed: 23163321]

67. Kondo T, Kawai T, Akira S. Dissecting Negative Regulation of Toll-like Receptor Signaling. Trends Immunol. 2012; 33:449–458. [PubMed: 22721918]

68. Hennessy EJ, Parker AE, O'Neill LAJ. Targeting Toll-like Receptors: Emerging Therapeutics? Nat Rev Drug Discov. 2010; 9:293–307. [PubMed: 20380038]

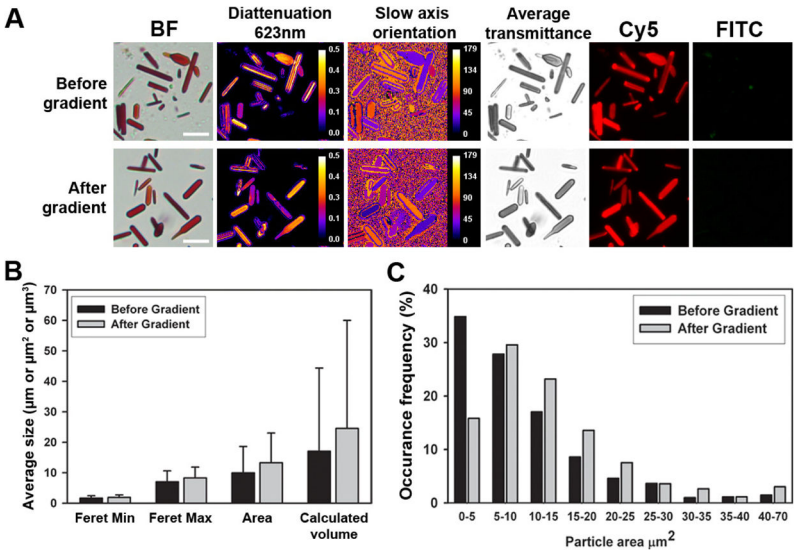

Figure 1.

Purification of CLDIs from the spleen of 8wk CFZ-fed mice using differential sucrose gradient centrifugation. (**A**) Brightfield (BF), polarized (diattenuation at 623 nm, slow axis orientation and average transmittance) and fluorescence (Cy5 and FITC) microscopy of spleen CLDIs before (top panel) and after (bottom panel) sucrose gradient centrifugation which shows the two were visually similar. (**B**) Average Feret max, min and area dimensions of CLDIs before (n=629) and after (n=531) sucrose gradient centrifugation. Average volume was calculated using area, Feret max and min values (also see supplemental figure S1). The data are the mean (± S.D.) of the total CLDIs analyzed. (**C**) Size (area) distribution of CLDIs before and after sucrose gradient centrifugation.

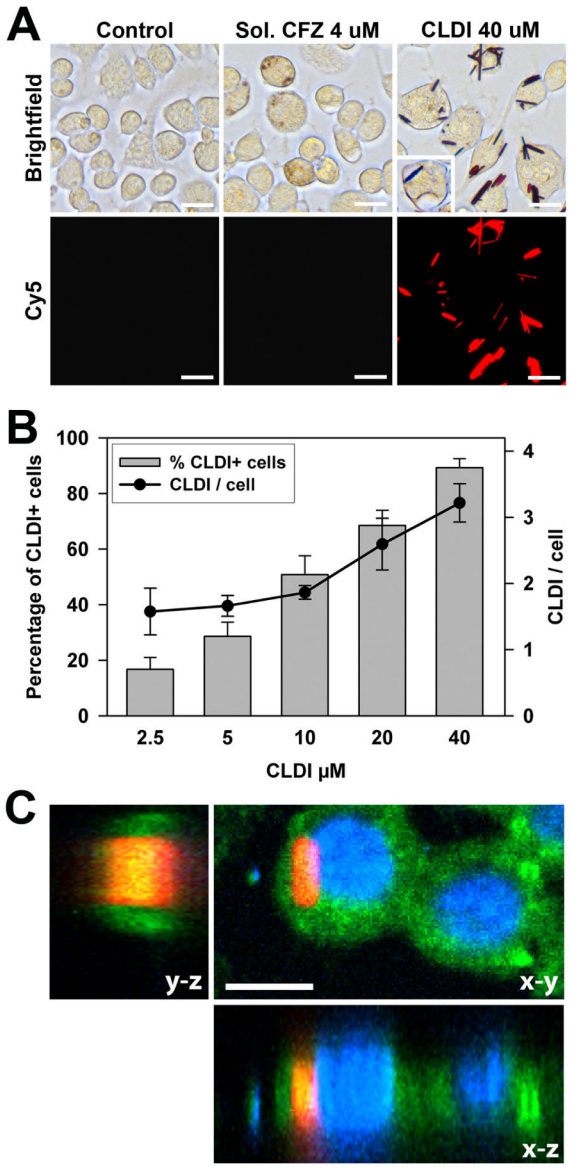

Figure 2.

Phagocytosis of soluble CFZ or CLDIs by RAW 264.7 cells. (**A**) Brightfield (top panel) and fluorescence (Cy5; lower panel) microscopy of RAW 264.7 cell that were incubated with soluble CFZ or CLDIs for 24h showing the presence of each CFZ species in the intracellular space. Inset image displays CLDI in vacuole-like intracellular vesicle. Bar = 20 µm. (**B**) Concentration dependent increases in the percentage of CLDI positive cells and the number of CLDIs per cell. Data are the mean (± S.D.) of cell percentage or CLDI number from 5 or 6 images acquired from two different experiments with at least 640 total cells per condition. Correlation analysis (Pearson's) of CLDI concentration versus CLDI phagocytosis showed strong associations ($r = 0.936$ for percentage of CLDI-positive cells, $p < 0.001$; $r = 0.912$ for CLDIs per cell, $p < 0.001$). (**C**) Composite Z-stack of confocal fluorescence images showing the intracellular location of a CLDI after incubation with RAW 264.7 cells. Shown are the y-

z (left), x-y (top right) and x-z (bottom right) projections of cell and CLDI in monolayer. Bar = 10 μm.

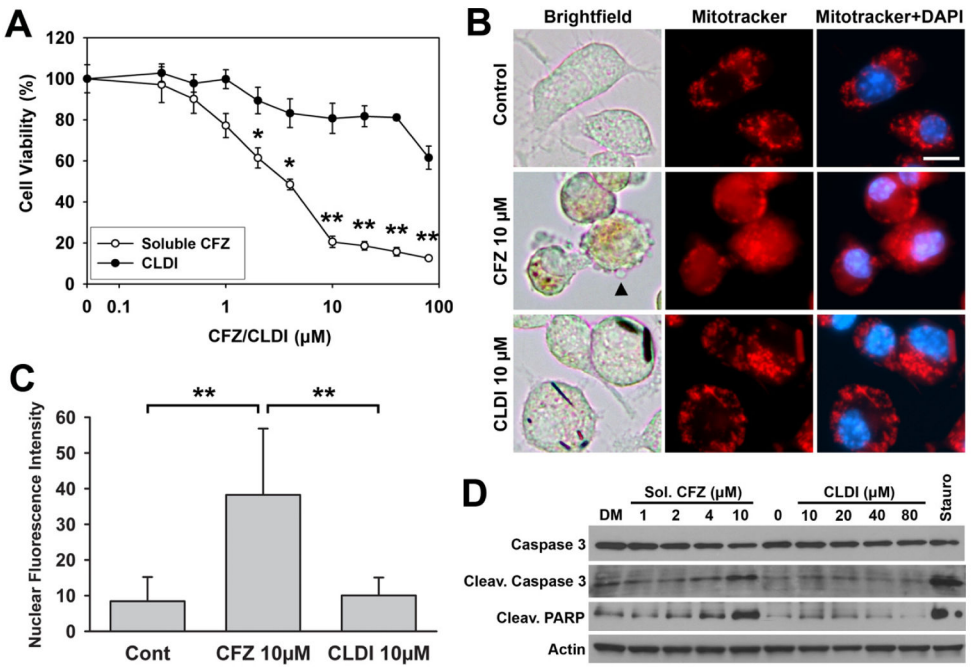

Figure 3.

Intracellular CLDIs are not cytotoxic to RAW 264.7 cells. (**A**) Increasing concentrations of soluble CFZ (○) lead to decreased cell viability as compared with CLDIs (●) measured by XTT assay. Data are the mean of triplicate wells ± S.D., representative of three independent experiments (* $p < 0.05$, ** $p < 0.01$; unpaired Student's t-test). (**B**) Mitotracker Red and NucBlue (DAPI) staining of control, soluble CFZ (10μM) and CLDI (10μM) treated RAW 264.7 cells shows dissipation of mitochondrial membrane potential in soluble CFZ-treated cells, evidenced by diffuse cytoplasmic Mitotracker staining (middle panel), but not in CLDI treated cells (bottom panel). Bar = 10 μm. (**C**) Quantification of mitochondrial membrane potential dissipation by measurement of nuclear fluorescence intensity of Mitotracker Red in control, CFZ (10μM) and CLDI (10μM) treated RAW 264.7 cells. Data are the mean ± S.D. of at least 80 cells per condition (** $p < 0.01$; ANOVA with Bonferroni's post-hoc tests). (**D**) Representative RAW 264.7 cell Western blot of caspase 3, cleaved caspase 3 and cleaved PARP following treatment with increasing concentrations of soluble CFZ or CLDIs for 24h. Exposure of cells to 4 and 10 μM of soluble (sol) CFZ resulted in increased caspase 3 and PARP cleavage, indicative of activation of apoptosis pathways, which was not evident in any of the CLDI treated cells. An untreated control (DMSO or 0) and cells treated with staurosporine (stauro; 500nM for 3h) were used as negative and positive controls, respectively.

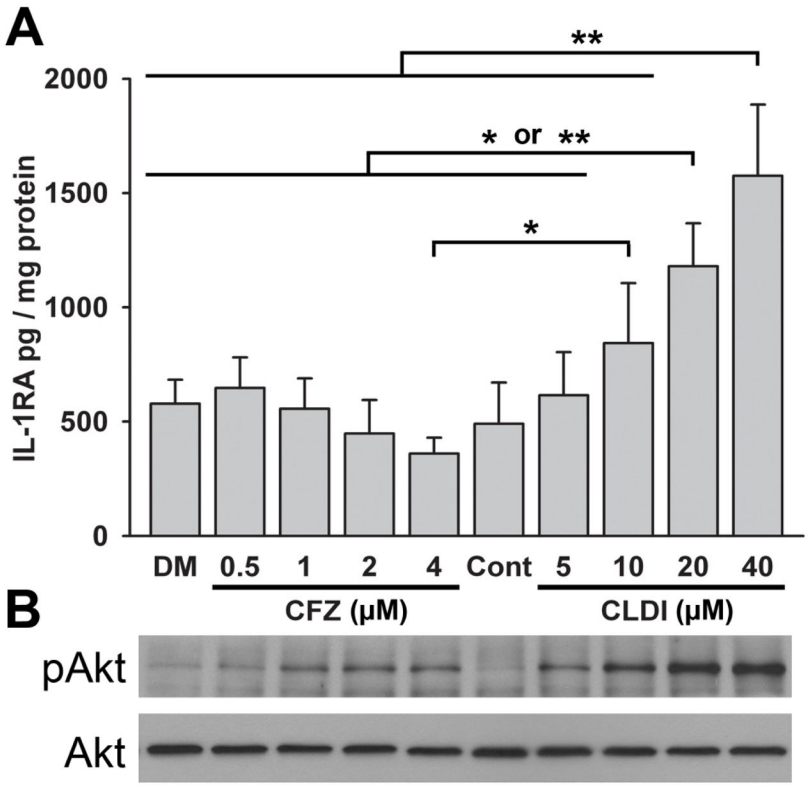

Figure 4.

Intracellular CLDIs enhance IL-1RA production and activate Akt in RAW 264.7 cells. (**A**) IL-1RA production in the media increased in CLDI containing cells compared with negative control cells (DM=DMSO) or cells containing intracellular CFZ. Data are the mean (± S.D.) IL-1RA pg per mg of cell protein concentration from three independent experiments. (* $p<0.05$, ** $p<0.01$; ANOVA with Bonferroni's post-hoc tests). Correlation analysis (Pearson's) between soluble CFZ and IL-1RA showed a negative association ($r = -0.637$, $p = 0.011$) and a positive association between CLDI and IL-1RA ($r = 0.896$, $p < 0.001$). (**B**) Representative RAW 264.7 cell Western blot of Akt phosphorylated at Ser473 (pAkt) and total Akt detected in the same cell lysates as those assayed for IL-1RA showing up regulation of pAkt with increasing CLDI concentration.

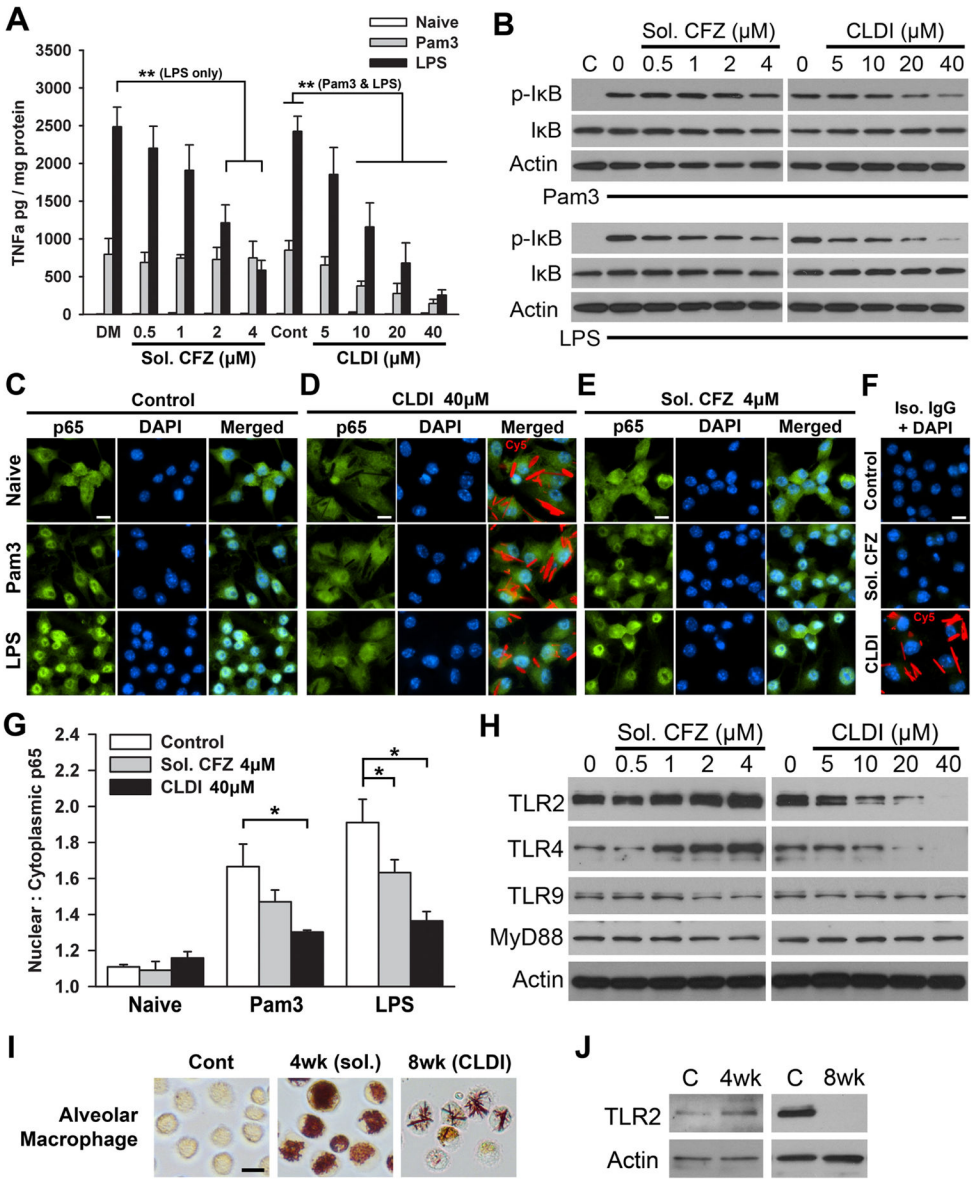

Figure 5.

Intracellular CLDIs dampen TLR2 and 4-mediated NF-κB activation and TNFα production in RAW 264.7 cells. (**A**) TNFα production from non-stimulated cells (naïve) or negative control cells (DM: DMSO or Cont) with or without intracellular soluble (sol.) CFZ or CLDIs following a 6h stimulation by the TLR2 agonist, Pam3 or the TLR4 agonist, LPS. Results show a CLDI-concentration dependent suppression of TNFα. Soluble CFZ modestly reduced Pam3- and LPS-induced TNFα production, which may be due in part, to loss of cell viability (see Figure 3A). Data are the mean (± S.D.) TNFα pg per mg of cell protein concentration from three independent experiments. Correlation analysis (Pearson's) showed no association between soluble CFZ and TNFα production in Pam3-stimulated cells (r = −0.018, p = 0.948) and negative association in LPS-stimulated cells (r = −0.941, $p < 0.001$). Correlation for CLDIs and TNFα showed strong negative correlation (r = −0.846 for Pam3;

$r = -0.886$ for LPS; both $p < 0.001$). (**B**) Representative Western blot of RAW 264.7 cell phosphorylated IκB (p-IκB) and IκB from naïve cells (c) or cells with or without intracellular soluble (sol.) CFZ or CLDIs in response to a 1h stimulation with Pam3 (top panel) or LPS (bottom panel). These data corroborate the data in (**A**) because intracellular CLDIs reduced both Pam3 and LPS-induced p-IκB. (**C**–**E**) Representative p65 and isotype IgG (**F**) immunofluorescence images displaying p65 nuclear translocation in control (**C**), 4μM soluble CFZ (**D**), or 40μM CLDI (**E**) treated cells non-stimulated (naïve) or stimulated with Pam3 or LPS for 3h. Images were used for p65 nuclear:cytoplasmic ratio measurements quantitatively presented in (**G**). These data show the ability of intracellular CLDIs to suppress both Pam3 and LPS induced p65 translocation to a greater extent than soluble (sol.) CFZ. Data are the mean (± S.D.) from analysis of 3 separate images (minimum 200 total cells per condition). (**H**) Representative Western blot of RAW 264.7 cell TLR2, TLR4, TLR9 and MyD88 expression in cells with or without intracellular soluble (sol.) CFZ or CLDIs demonstrating the CLDI-induced down regulation of TLR2 and TLR4. (**I**) Brightfield images displaying mouse primary alveolar macrophages isolated from mice fed with control diet or CFZ for 4 wks (contains soluble CFZ) or 8 wks (contains CLDI), and (**J**) detection of TLR2 by Western blot shows reduced expression of TLR2 in alveolar macrophages from 8 wk CFZ-fed mice, while 4wk CFZ-fed mice show increased levels of TLR2 compared to control alveolar macrophages. (* $p < 0.05$, ** $p < 0.01$; ANOVA with Bonferroni's post-hoc tests).